

# Ultra-wideband chaotic radio pulse reception in the case of inter-pulse interference

Lev Kuzmin<sup>1\*</sup> and Alexander Grinevich<sup>2</sup>

<sup>1</sup>Kotelnikov Inst. of Radio Engineering and Electronics, 125009 Mokhovaya st., 11/7, Moscow, Russia

<sup>2</sup>Bauman Moscow State Technical University, 105505, Baumanskaya 2-ya st., 5, Moscow

**Abstract.** The problem of receiving ultra-wideband (UWB) chaotic radio pulses of microwave band that passed through a multipath channel is considered. Based on measurements of UWB chaotic radio pulse propagation through a real wireless channel, a method for reception is proposed that is not affected by interpulse interference.

## 1 Introduction

A method for blind energy detection of ultra-wideband (UWB) chaotic radio pulses of microwave band that is not affected by interpulse interference due to multipath propagation of the UWB signal [1] is proposed. The method is blind, since it does not require sounding of the multipath channel.

Noncoherent detection of chaotic radio pulses in a multipath channel is not a problem when the propagation delays of the reflected paths do not exceed the duration of the interpulse guard interval [2–4]. In such a case, there is actually no interpulse interference, thus, the performance of energy detection of chaotic radio pulses in the multipath channel in terms of error probability is close to that of AWGN single path channel [2, 3].

Problems with coherent and noncoherent detection of UWB signals appear for both chaotic UWB radio pulses [5, 6] and ultrashort UWB pulses [7], if the delays of the reflected path go beyond the limits of the interpulse guard interval, which is typical, e.g., for mobile wireless systems. To solve this problem, the following methods were proposed and investigated: energy detection using *a priori* statistical estimation of a multipath UWB channel parameters [5, 7], blind energy detection [8–12], and RAKE methods ([13, 14] and references therein) for ultra-short pulses. In the case of UWB RAKE receivers, methods of selecting paths based on PRAKE (partial RAKE), SRAKE (selective RAKE) schemes [13], and their modifications [14] were considered. It was found that in terms of error probability, such RAKE receivers have the same or lower theoretical performance, at minimum, as compared with energy receivers, but are inferior in simplicity of implementation. This is due to the large number of paths in the UWB channel, which can have approximately the same power [14, 15] and the reception of UWB signals must be carried out for all such paths.

---

\* Corresponding author: [lvkuzmin@gmail.com](mailto:lvkuzmin@gmail.com)

In this paper an approach for detecting a sequence of chaotic UWB radio pulses against the background of interspersed interference using blind energy detection is proposed. The method is based on a natural property of the chaotic UWB signal: noncoherent summation of all the paths coming in the receiver input, which eliminates the problem of extracting the most powerful paths as in the RAKE receiver. The method is analyzed on an array of experimental data on propagation of such pulses with duration  $T_p = 83$  ns and repetition period  $T = 166$  ns (i.e., the pulses are separated by  $(T - T_p) = 83$  ns pause intervals) through a wireless channel.

The interspersed interference power is assumed to be greater than the thermal noise power of the receiver, so the latter can be neglected. This is a fair assumption, since otherwise, given the limited sensitivity of a real receiver, it will not be able to detect the multipath signal against the thermal noise [6], and it would be meaningless to consider the task posed.

## 2 Experiment

In the experiment according to layout in fig. 1a, interspersed interference was observed in  $R_X$  reception point in a real wireless channel, where  $R_X$  receiver was stationary and  $T_X$  emitter was moved, so that the distance between the receiver and emitter  $r$  had the following values:  $r_1 = 32$ ,  $r_2 = 16$ ,  $r_3 = 8$ ,  $r_4 = 4$ , and  $r_5 = 2$  m.

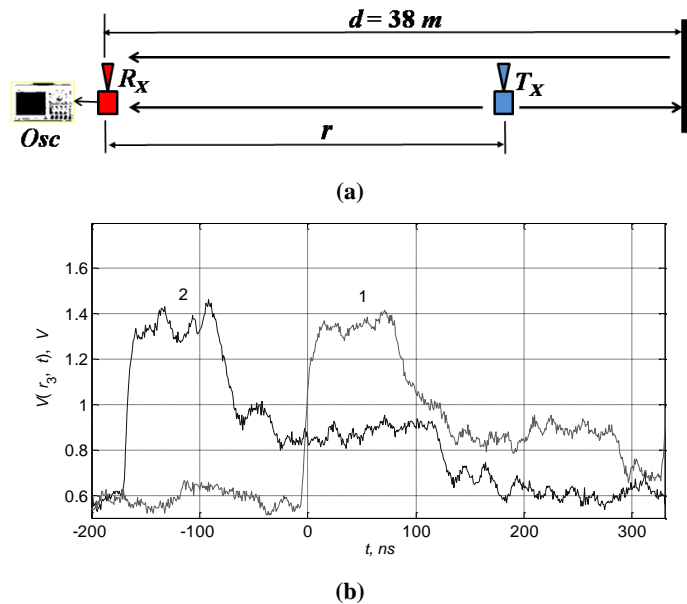


**Fig. 1.** Measurements of the propagation characteristics: (a) experimental layout.  $R_X$  – receiver,  $T_X$  – emitter,  $Osc$  – oscilloscope,  $d = 38$  m,  $r$  is varied in the range 2 to 32 m; (b) envelopes of chaotic radio pulses  $V(r_3, t)$  for  $r_3 = 8$  m illustrating interspersed interference in the receiver: curve 1 is the envelope of the current pulse to be detected, 2 is the envelope of the preceding pulse.

As is shown in [6], such a measurement scheme creates conditions necessary for the appearance of interspersed interference and allows us to observe two paths in the experiment: the direct one (line of sight) and a path reflected from a massive metal door in the end of the corridor, where the experiment is conducted [6]. Emitter  $T_X$  forms a sequence of  $N_3 \approx 100$  chaotic radio pulses, and receiver  $R_X$  forms the envelope of the received pulses. A storage oscilloscope samples and records the envelope signal at 2.5 GHz sampling rate. The appearance of interspersed interference is illustrated in Fig. 1b on example of two envelopes

for two consecutive pulses  $V_j(r_3, t), j = 1 \dots N_3$ , taken at a fixed distance  $r_3 = 8 \text{ m}$  between the transmitter and the receiver, in which case two radio pulses are delayed by the duration of guard interval. Interpulse interference is manifested in overlapping of the positions of the current pulse (curve 1), that is to be detected, and the previous pulse (curve 2).

Rx receiver consisted of a log-detector [15] and a low-noise amplifier with gain 100. The receiver in its operation range converts the input power varying from  $3 \cdot 10^{-9} \text{ mW}$  to  $\sim 1 \text{ mW}$  to an output voltage in the range 0.5 to 2 V according to the following expression

$$V(r, t) = 10\alpha \lg(P(r, t) / P_0), \quad (1)$$

where  $P_0 = 1 \text{ mW}$ ;  $\alpha = 0.021 \text{ V/dB}$  is log-detector slope;  $P(r, t)$  is the power of the signal at the receiver input from an emitter located at distance  $r$ . Due to logarithmic rule of power-to-voltage conversion, the amplitude of the signal envelope at the receiver output varies linearly, while the signal power at the input can vary by several orders of magnitude.

Using such a receiver, a detection method is proposed that requires no a priori determination of the threshold  $H$ , necessary to make decision on the arrival or on the absence of the pulse in one-path channel [4]. If the channel power exceeds the power threshold  $H$ , this means the arrival of the pulse. Threshold  $H$  is fixed and it is determined by the total power of the receiver thermal noise and the power of the interfering signal arising from the technical implementation errors.

In this paper, the task of designing a blind rule for deciding whether a pulse has arrived or not against the background of interpulse interference is analyzed in a situation when the receiver gets a “pulse-pause-no pulse” signal. In this case, there is a non-zero probability of “receiving” the absent pulse (“false alarm”) after a pause, if the threshold value of the power  $H$  is set as it is done in a single-beam channel. In the cases: “pulse-pulse-pulse”, “no pulse-pulse-pulse”, and “no pulse-pulse-no pulse” the wrong detection does not occur when using a fixed threshold  $H$ .

To prevent wrong detections, it is proposed to use the knowledge of the reflected signal attenuation pattern, which passes a greater path than the direct beam before coming to the receiver, therefore: (1) its power is obviously less than the power of the direct path, (2) the upper boundary of this power can be estimated, knowing the pulse repetition frequency, the attenuation rate of the signal in the channel, and the fact that the paths in the receiver are summed incoherently due to small autocorrelation time of the chaotic signal [6]. These parameters do not depend on the conditions of signal propagation in each specific case; therefore the proposed method is blind.

In the wireless channel, the signal power  $P_R$  in the reception point is proportional to  $\sim P_T / r^n$  [1], where  $n = n_0 = 2$  for free space and  $n = n_1 < 2$  in the multipath channel with direct path. In the case of no direct path, one can expect that  $n = n_2 > 2$ , moreover,  $n = n_2 \geq 2n_1$ , since this is a re-reflected signal.

Here, the pathloss exponent of the re-reflected signal was determined experimentally similar to [6], where the pathloss exponent for the direct path was measured, which turned out to be equal to  $n_1 \approx 1.5$ . For the experimental determination of the pathloss exponent value of the re-reflected rays with method [6], the averaged shape of the pulse envelope

was calculated as  $\langle V(r_i, t) \rangle = (1/N_i) \sum_{j=1}^{N_i} V_j(r_i, t)$ . The resulting averaged forms  $\langle V(r_i, t) \rangle$

for pulses with 100-mW emission power for  $r_5 = 2, r_4 = 4, r_3 = 8, r_2 = 16$  and  $r_1 = 32 \text{ m}$  are shown in Fig. 2a.

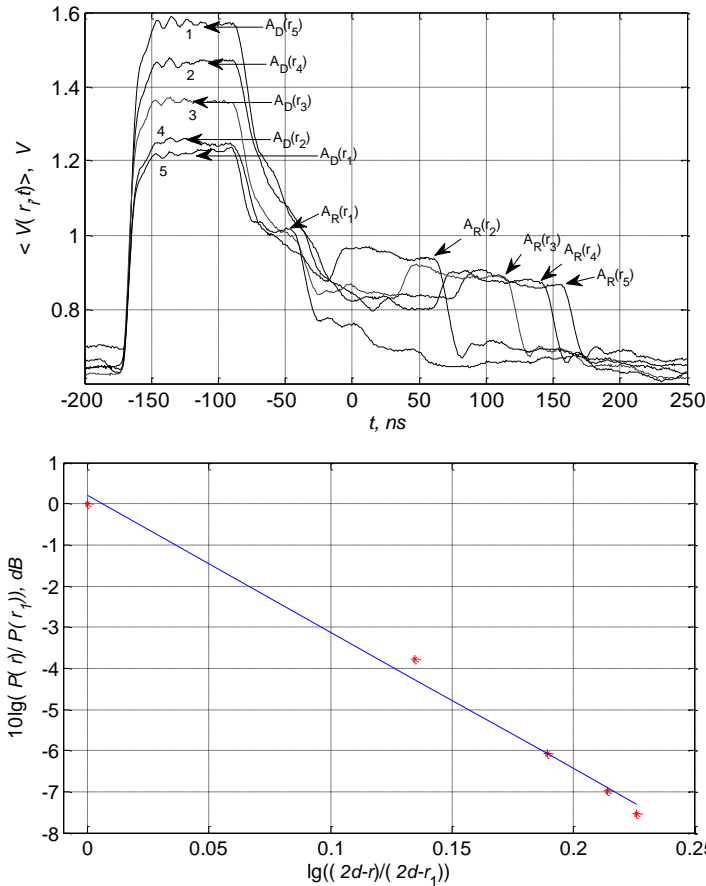


**Fig. 2.** (a) Average pulse envelope waveforms  $\langle V(r_i, t) \rangle$ , on which the average amplitudes of the direct  $\langle A_D(r_i) \rangle$  and reflected  $\langle A_R(r_i) \rangle$  paths recorded by the receiver at distance  $r_i$  (m) from the emitter for pulses with 100-mW power are marked:  $\langle A_R(r_5 = 2) \rangle = 0.85$  V (curve 1),  $\langle A_R(r_4 = 4) \rangle = 0.86$  V (curve 2),  $\langle A_R(r_3 = 8) \rangle = 0.88$  V (curve 3),  $\langle A_R(r_2 = 16) \rangle = 0.93$  V (curve 4),  $\langle A_R(r_1 = 32) \rangle = 1.01$  V (curve 5); and (b) a plot of the power ratio  $P(r) / P(r_1)$  for the reflected path in dB as a function of the distance ratio  $\lg((2d-r) / (2d-r_1))$ ; crosses mark measurement results, solid line is approximation.

The upper curve 1 in Fig. 2a corresponds to the minimum distance between the emitter and receiver, and the lower curve 5 corresponds to the maximum distance. Average amplitudes of the reflected path pulses  $\langle A_R(r_i) \rangle$  were determined from the average envelopes  $\langle V(r_i, t) \rangle$ . The signal power attenuation rate at distance  $r_i$  for reflected paths was calculated with expression (1) using the difference between the pulse amplitude for distance  $r_1$  and distance  $r_i$ :  $\langle A_R(r_i) \rangle - \langle A_R(r_1) \rangle \approx 10\alpha \lg(P_R(r_1) / P_R(r_i))$ . Since the ratio of the power of the reflected path at distance  $r_1$  to the power  $P_R(r_i)$  at distance  $r_i$  is  $P_R(r_1) / P_R(r_i) = ((2d - r_i) / (2d - r_1))^{n_2}$ , then:

$$(\langle A(r_i) \rangle - \langle A(r_1) \rangle) / \alpha = 10n_2 \lg((2d - r_i) / (2d - r_1)) \tag{2}$$

Using the experimental dependence of  $(\langle A(r_i) \rangle - \langle A(r_1) \rangle)$  on  $\lg((2d - r_i)/(2d - r_1))$ , attenuation power  $n_2$  was determined from the slope of line (2), which approximated the experimental data (Fig. 2b). The pathloss exponent value turned out to be equal to  $n_2 = 3.3$  for the reflected path, which is consistent with the estimate  $n_2 \geq 2n_1$ ,  $n_1 \approx 1.5$ .

Based on the regularity of the power drop of the reflected path with the path length, it is possible to calculate the threshold value of power  $H$ , above which the receiver detects only a direct path and which the reflected path doesn't exceed by all means, i.e., to implement blind detection of chaotic radio pulses on the direct path.

The threshold  $H$  is calculated on the basis of the pulse repetition period  $T$  and the pathloss exponents  $n_1$  and  $n_2$  of the direct and reflected paths, respectively. Since the power

of the direct path in the receiver is  $P_D = P_T \left( \frac{c}{4\pi f r_D} \right)^{n_1}$ , and the power of the reflected one is

$P_{RT} = \gamma P_T \left( \frac{c}{4\pi f (r_D + cT)} \right)^{n_2}$ , where  $\gamma$  is the power reflection fraction,  $f$  is the average

frequency of the signal,  $c$  is the light speed,  $r_D$  is the length of the direct path,  $cT$  is the path surplus of the beam that will occur on current position of the chaotic radio pulse in time  $T$  after the previous one, then the power limit  $P_{RT}^*$  for the reflected path in the receiver can be obtained from the ratio  $P_{RT} / P_D$  in time  $T$  after the direct path arrival. For  $n_2 = 2n_1$ , we have

$$P_{RT}^* = \gamma P_D \left( \frac{c}{4\pi f r_D} \right)^{n_1} \left( \frac{1}{1 + cT / r_D} \right)^{2n_1} \quad (3)$$

For the value of  $n_1$  in  $P_{RT}^*$  (3), one can take  $n_1 = 1.6$ , which is consistent with other experimental data on measurements of UWB channel parameters [1]. The value of  $\gamma$  can be set to  $\gamma = 1$  (total reflection), and for the relation  $cT / r_D$ , one can assume that  $cT / r_D \ll 1$  (the worst case).

As a result, the detection of a direct path against the reflection background should be carried out with a threshold value  $H > P_{RT}^*$ . The value  $P_{RT}^*$  (3) is calculated based on the average values of the amplitudes of the chaotic radio pulse envelope based on the direct and reflected paths. At the same time, the amplitudes of the chaotic radio pulses in the sequence envelope vary from pulse to pulse according to a certain distribution. Therefore, to prevent errors caused by the spread of the incoming pulses' power, it is also necessary to take into account the width of these distributions. Fig. 3 shows the experimental distributions of the pulse envelope amplitudes for the direct and reflected paths. The distributions are limited: the amplitude spread is within  $\pm 0.1$  V of their average values. This means that the detection of a direct beam against the reflected one can be performed with a threshold power value  $H > P_{RT}^* + \Delta P_{RT}$ , where  $\Delta P_{RT} = 0.1/\alpha$ .

As a result, there is a physical opportunity to eliminate the influence of interpulse interference and to achieve detection characteristics that are close in error probability to a channel with one direct path without implementing the procedure of individual path allocation carried out in RAKE receiver.

The work was performed according to the state assignment of Kotelnikov IRE RAS.

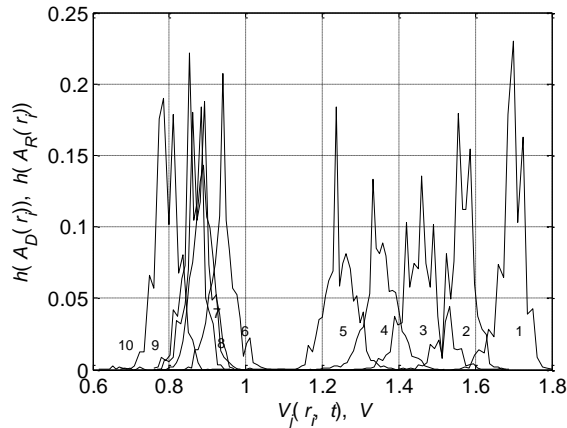


**Fig. 3.** Distributions of amplitudes for direct  $h(A_D(r_i))$  (curves 1 –  $r_1 = 32$  m, 2 –  $r_2 = 16$  m, 3 –  $r_3 = 8$  m, 4 –  $r_4 = 4$  m, 5 –  $r_5 = 2$  m) and reflected path pulses  $h(A_R(r_i))$  (curves 6 –  $r_5 = 2$  m, 7 –  $r_4 = 4$  m, 8 –  $r_3 = 8$  m, 9 –  $r_2 = 16$  m, 10 –  $r_1 = 32$  m).

## References

1. A.F. Molisch, Proc. of the IEEE **97**, 353–371 (2009).
2. Yu.V. Andreyev, A.S. Dmitriev, E.V. Efremova, A.D. Khilinsky, L. V. Kuzmin, Int. J. Bifurcation and Chaos **15**, 3639–3651 (2005).
3. L.V. Kuz'min, J. Commun. Technol. El+ **56**, 399–416 (2011).
4. A.S. Dmitriev, A.I. Ryzhov, M.G. Popov, Radioelectronics. Nanosystems. Information Technologies. (RENSIT) **10** 313–322 (2018).
5. L. V. Kuz'min, V. A. Morozov, J Commun Technol El+ **54** 313–322 (2009).
6. Kuz'min, L.V., Grinevich, A.V. & Ushakov, M.D. J. Commun. Technol. El+ **64**, 787–796 (2019).
7. K. Witrisal, G. Leus, G.J.M. Janssen, M. Pausini, F. Troesch, T. Zasowski, J. Romme, IEEE Signal Processing Magazine **26** 48–66 (2009).
8. H. Ma, X. Wang, Y. Lu, L. Tian, IEEE Int. Conf. on Smart Grid and Smart Cities (ICSGSC) 308-311 (2017).
9. E. Arias-de-Reyna, J. J. Murillo-Fuentes, R. Boloix-Tortosa, IEEE Signal Processing Lett. **22** 2019-2023 (2015).
10. B. Shen, R. Yang, T. Cui, K. Kwak, IEEE Int. Conf. on Ultra-Wideband 1–4 (2010).
11. W. Wu, IEEE Int. Conf. on Ultra-Wideband 556–561 (2007).
12. A. F. dos Santos, W. Rave, G. Fettweis, IEEE Int. Conf. on Ultra-Wideband 41–44 (2008).
13. D. Cassioli, M. Z.Win, F.Vatalaro, A. F. Molisch, IEEE Trans. on Wireless Communications **6** 1265–1275 (2007).
14. N. B. Benotmane, S. A. Elahmar, I. Dayoub, W. Hamouda, IEEE Trans. on Vehicular Technology **67** 7749–7753 (2018).
15. Analog Devices, Data Sheet 1 MHz to 4 GHz, 80 dB, Logarithmic Detector/Controller, <http://www.analog.com/media/en/technical-documentation/data-sheets/ADL5513.pdf>